Amplification of *PVT1* contributes to the pathophysiology of ovarian and breast cancer

Yinghui Guan[1], Wen-Lin Kuo[1], Jackie L. Stilwell[2], Hirokuni Takano[3], Anna V. Lapuk[1], Jane Fridlyand[4], Jian-Hua Mao[5], Mamie Yu[6], Melinda E. Miller[7], Jennifer L. Santos[8], Steve E. Kalloger[9], Joseph W. Carlson[1], David G. Ginzinger[3], Susan E. Celniker[1], David G. Huntman[9], Joe W. Gray[1,2]

[1]Life Sciences Division, Lawrence Berkeley National Laboratory, Berkeley, CA; [2]Trubion Pharmaceuticals, Seattle, WA; [3]Department of Laboratory Medicine, University of California, San Francisco, San Francisco, CA; [4]Genentech Inc., South San Francisco, CA; [5]Cancer Research Institute, University of California, San Francisco, San Francisco, CA; [6]Department of Neurosurgery Research, University of California, San Francisco, San Francisco, CA; [7]Centre for Translational and Applied Genomics, Vancouver BC, Canada; [8]Cheryl Brown Ovarian Cancer Outcomes Unit of the British Columbia Cancer Agency, Vancouver BC, Canada; [9]Department of Pathology, University of British Columbia, Vancouver General Hospital and British Columbia Cancer Agency, Vancouver BC, Canada

Financial Support: This work was supported in part by the U.S. Department of Energy, Office of Science, Office of Biological and Environmental Research (Contract DE-AC03-76SF00098) and by the National Institutes of Health, National Cancer Institute grants CA 58207, CA 83639 and CA 64602 to JWG.

Corresponding author:
Joe W Gray
Life Sciences Division, Lawrence Berkeley National Laboratory, One Cyclotron Rd. MS977/225A, Berkeley, CA94720, USA
Phone: (510)495-2438, Fax: (510) 495-2535 e-mail: jwgray@lbl.gov

Running Title: *PVT1* amplification in cancer

Keywords: microarray, ovarian cancer, 8q24, *MYC*, *PVT1*

ABSTRACT

Purpose. This study was designed to elucidate the role of amplification at 8q24 in the pathophysiology of ovarian and breast cancer since increased copy number at this locus is one of the most frequent genomic abnormalities in these cancers. **Experimental Design.** To accomplish this, we assessed the association of amplificaiton at 8q24 with outcome in ovarian cancers using FISH to tissue microarrays and measured responses of ovarian and breast cancer cell lines to specific small interfering RNAs (siRNA) against the oncogene, *MYC,* and a putative noncoding RNA, *PVT1*, both of which map to 8q24. **Results.** Amplification of 8q24 was associated with significantly reduced survival duration. In addition, siRNA-mediated reduction in either *PVT1* or *MYC* expression inhibited proliferation in breast and ovarian cancer cell lines in which they were both amplified and over expressed but not in lines in which they were not amplified/over expressed. Inhibition of *PVT1* expression also induced a strong apoptotic response in cell lines in which it was over expressed but not in lines in which it was not amplified/over expressed. Inhibition of *MYC*, on the other hand, did not induce an apoptotic response in cell lines in which *MYC* was amplified and over expressed. **Conclusions**. These results suggest that *MYC* and *PVT1* contribute independently to ovarian and breast pathogenesis when over expressed because of genomic abnormalities. They also suggest that *PVT1* mediated inhibition of apoptosis may explain why amplification of 8q24 is associated with reduced survival duration in patients treated with agents that act through apoptotic mechanisms.

INTRODUCTION

Amplification of a region on chromosome 8q24 is one of the most frequent events in carcinomas including serous ovarian and breast cancers and has been associated with reduced survival duration in some studies (1, 2). The well-established oncogene, *MYC*, maps to this locus and likely contributes to the pathophysiology of cancers in which it is amplified. However, the *PVT1* transcript also maps to this region and has been implicated in cancer pathophysiology as well (3). In mouse, for example, the *pvt-1* locus is a site of recurrent translocation in plasmacytomas (4, 5) and is a common site of tumorigenic retroviral insertion in lymphomas (6). In humans, the region homologous to *pvt-1* is a site of recurrent translocation between chromosomes 2 and 8 (7, 8) and its first exon is co-amplified with *MYC* in colon carcinoma cell lines (9). *PVT1* has been suggested as a *MYC* activator (10), however, little evidence exists to support that role. Moreover, evidence is now emerging that *PVT1* may act as a noncoding RNA (Huppi et al., private communication) that is strongly conserved between mouse and human.

We now present evidence that both *PVT1* and *MYC* contribute to ovarian and breast cancer pathophysiology when over expressed by amplification at 8q24. First, we show that amplification at this locus is associated with reduced survival duration in ovarian cancer. We also show that down-regulation of either *PVT1* or *MYC* expression using small interfering RNA (siRNA) technology inhibits proliferation in ovarian and breast cancer cell lines in which they are amplified and over expressed but not in cell lines in which they are not over expressed. In addition, we show that inhibition of *PVT1* but not *MYC* induces an amplification/over expression-specific apoptotic response. Our analyses of *PVT1* transcripts are consistent with the interpretation that *PVT1* exerts its pathophysiological influence as a noncoding RNA (Private communication with Dr. Konrad Huppi).

MATERIALS AND METHODS

Cancer cell lines. Ovarian cancer cell lines with and without amplification at 8q24 were selected from a collection of 30 cell lines that were either purchased from ATCC, European Collection of Cell Culture (ECCC), DSMZ-the German Resource Centre for Biological Material (DSMZ) and Interlab Cell Line Collection (ICLC) or generously provided by Dr. Gordon Mills and Dr. Robert Bast, MD Anderson Cancer Center (MDA), Dr. Tom Hamilton in Fox Chase Cancer Center (FCCC), Dr. Nelly Auersperg in University of British Columbia (UBC) and National Cancer Institute (NCI) Drug Panel (listed in Table S1). The known biological properties of the cell lines are summarized in Table S1. Breast cancer cell lines with and without amplification at 8q24 were selected from a collection of 51 well-characterized lines described by Neve et al. (11).

Nucleic acid extraction. Genome DNA and total RNA were purified from cultured cells as described previously (11). Total RNA from a panel of normal human tissues was purchased from Clontech (catalogue number: 636643) and used to measure relative expression levels of *PVT1*.

Genome copy number and expression analysis. Relative genome number was assessed in the 30 ovarian cell lines using array CGH with three BAC arrays as described previously (12, 13). These included: (a) Hum2.0 arrays comprised of 2465 BACs selected at approximately megabase intervals along the genome (12, 14). (b) Arrays comprised of 1860 BACs selected to include genes known to be involved in cancer pathogenesis (15). (c) Arrays carrying 400 BACs selected to tile across 13 Mbp at 3q26, 15 Mbp at 8q24, and 30 Mbp at 20q centered on regions of recurrent amplification associated with reduced survival

duration in earlier studies (15). Global gene expression was assessed by hybridization to Affymetrix U133A arrays in the J David Gladstone Institutes in University of California, San Francisco as described (www.affymetrix.com). Hybridized arrays were visualized with Affymetrix Microarray Suite 5.0® (MS5.0). The image files of all the arrays were then analyzed together with the robust multiarray average (RMA) algorithms (16). Genome copy number and expression analyses of the breast cancer cell lines used in this study are described by Neve et al.(11).

Real-time Quantitative-PCR (QPCR) Analysis. QPCR was performed essentially as described previously (17). Quantitative detection of specific nucleotide sequences was based on the fluorogenic 5' nuclease assay and relative expression was calculated as described (17). Assays were purchased as Assays–on-Demand from Applied Biosystems. The catalogue numbers of these assays are listed in Table S2. The sequences of PCR primers and Taqman probe specific for *PVT1* transcription unit were designed with ABI Primer Express 2.0 software based on the sequence of a published expressed sequence tag (EST) clone for human *PVT1* (NCBI accession number: M34428). The primer sequences for PVT1 were: sense-CATCCGGCGCTCAGCT, antisense-TCATGATGGCTGTATGTGCCA. The Taqman probe was 5'-FAM-CTGACCATACTCCCTGGAGCCTTCTCC-BHQ1-3'. Primer and probe concentrations of 500 nM and 200 nM, were used respectively. "No reverse transcriptase" analyses were performed on all samples to confirm that genomic DNA was not present. For normalization, cDNA equivalent to the amount of RNA used in target gene measurements was measured for ribosomal 18S, glyceraldehyde-3-phosphate dehydrogenase (GAPDH) and cyclophilin A.

Transfection of siRNA. siRNAs against *PVT1* and *MYC* were either designed using the 'Biotool' function available at www.idtdna.com and purchased from Integrated DNA Technologies (IDT,

Coralville, IA) or ordered from Dharmacon (Lafayette, CO) pre-designed siGENOME™ Collection. Two siRNAs cognate to different parts of mRNA sequence of *PVT1* (siPVT1a and siPVT1b) and two siRNAs cognate to different parts of *MYC* (siMYCa and siMYCb) were used in this study. The target sequence of si*PVT1a* was 5'-CAGCCATCATGATGGTACT-3' and that of siPVT1b was 5'-GGCACATTTCAGGATACTA-3'. The target sequence of siMYCa was 5'-GAGGCGAACACACAACGUC-3'. siMYCb was predesigned by Dharmacon (siGENOME ON-TARGET™ duplex 17, MYC, catalogue # D-003282-17) and its target sequence was 5'-GGACTATCCTGCTGCCAAG-3'. CY3 conjugated siRNA against *Aequorea* green fluorescent protein (siGFP) was designed and synthesized by IDT and used as a control for both transfection efficiency and non-sequence-specific siRNA effects. A pre-designed control siRNA (siControl) from Dharmacon (catalogue # D-001206-02-05) was also used as a second non-sequence-specific effect control.

Approximately $5x10^4$ cells were plated to each well of a 24-well plate at least 24 hours (h) before transfection in order to achieve 50-70% confluency. siRNA transfection was performed with Lipofectamine 2000® (Invitrogen, Carlsbad, CA) following manufacture's instructions. Cells were harvested or fixed 8, 24 and/or 48 h after transfection for RNA, protein, cell cycle distribution, cell viability and apoptosis analyses.

MYC Western Blotting. 10 μg of total protein sample was resolved in a pre-cast NuPage™ 4-12% Bis-Tris Gel (Invitrogen), electrophoresed at 200 volts for 45 minutes (min) and transferred to a piece of Immobilon™ transfer membrane at 250 mÃ for 50 min. Each membrane was then blocked and incubated with a monoclonal anti-*MYC* antibody (clone 9E10, sc-40, Santa Cruz Biotechnologies, Inc., Santa Cruz, CA) at room temperature for 1 h or at 4 ºC for overnight. Each blot was washed and incubated in buffer containing an anti-mouse IgG antibody (1:20,000) at room temperature for 1 h. Finally, each blot was

soaked in ECL chemiluminescent reagents (GE global research, Niskayuna, NY) for 1 min and exposed to an X-ray autoradiography film for 1 min-1 h.

BrdUrd DNA Analysis. The effects of siRNAs on cell cycle were assessed by measuring BrdUrd incorporation during a 30 min pulse two days after siRNA transfection. Cells were pulsed with 10μl of 1mM stock BrdUrd added to 1ml culture media in each well of a 24-well plate. Cells were subsequently trypsinized, fixed in 70% ethanol (EtOH) and stored in 4 ºC for at least 1 h. The cells were pelleted, resuspended in 0.08% pepsin (in 0.1 N HCl) and incubated at 37 ºC for 20 min to free nuclei. 2N HCl was then applied to nuclei to denature double stranded DNA and neutralized with 2 volumes of 0.1M sodium borate. The nuclei were then incubated on ice with 1:5 dilution of an FITC labeled anti-BrdUrd antibody (Becton Dickinson Immunocytometry Systems, San Jose, CA) for at least 30 min and stained with 50 μg/ml of PI at 37 ºC for at least 15 min. BrdUrd/DNA distributions were measured in a Becton Dickinson FACaliber flow cytometer (FACS). Alternately, cells were fixed with 70% EtOH after 30 min of BrdUrd labeling for at least 2 h in room temperature, stained with mouse anti-BrdUrd antibody (BD Biosciences, catalogue# 555627) and Alexa Fluor® 488 goat anti-mouse (Invitrogen, #A110001) antibody and counterstained with Hoechst 33342 (Sigma-Aldrich, St. Louis, MO). Cells were scanned and recorded using a Cellomics High Content Imaging system (Cellomics, KineticScan) (18). Both flow and image data were analyzed to determine the fractions of G_1, BrdUrd incorporating S-phase and G_2M cells as described (11, 18).

Apoptosis. The apoptotic effect of siRNA silencing was assessed using high content image analysis. At each time point, cells were either directly stained with 1μM YO-PRO®-1 stain (Invitrogen) and 10μg/ml Hoechst 33342 for 30 min at 37ºC or fixed in 4% formaldehyde at room temperature and stained with

Alexa Fluor 488-phalloidin (Invitrogen) for F-actin and10μg/ml Hoechst 33342 for nuclei. Apoptotic cells were detected and analyzed using Cellomics' Multiparameter Apoptosis and Multiparameter Cytotoxicity Bioapplications (Cellomics, Pittsburgh, PA) for F-actin content and Yo-Pro®-1 DNA staining, respectively. Intensities of YO-PRO®-1 and F-actin in cells treated with siRNA were analyzed and compared with those of cells treated with Lipofectamine only or siGFP and siControl with appropriate Cellomics applications. Significance was determined using a Student *t*-test.

Viable cell count analysis. Cell number was measured at 8 h, 24 h and/or 48 h after treatments using the CellTiter-Glo® Luminescent assay (Promega, Madison, WI) (CTG) according to manufacturer's instructions and luminescence was recorded with a luminometer (BioTek FLx800, BioTek Instruments, Inc., Winooski, VT).

5' Rapid amplification of cDNA ends (5'RACE) for determination of *PVT1* transcript structure The 5' N-terminal sequences of *PVT1* transcripts were determined using 5'RACE with total RNA from epithelial cells surgically scraped from normal ovary surface epithelium (OSE1157), an OSE cell line with extended life span in culture due to the transfection of SV40 large T antigen (IOSE29) and two immortalized ovarian cancer cell lines, CAOV4 and HEY. The reactions were carried out using a FirstChoice® RLM-RACE Kit (Ambion, Austin, TX) following the manufacturer's instructions. Single band PCR products from 5'RACE were gel purified and cloned using a TOPO TA cloning kit (Invitrogen: K4500-01). Plasmids containing the desired 5'RACE PCR product were isolated and purified from single bacterial colonies. They were then sequenced with M13 forward and reverse sequence primers. The sequences of individual *PVT1* exons were queried on http://microrna.sanger.ac.uk/sequences/search.shtml for potential stem-loop' structures commonly observed in micro RNAs (miRNA) (19, 20).

RESULTS

Genome copy number and transcriptional analyses. We applied fluorescence in situ hybridization (FISH; Figure 1a) for analysis of 380 ovarian tumors arranged in tissue microarrays with probes to the MYC locus (8q24) and the chromosome 8 centromere. This analysis showed that a MYC locus copy number to centromere copy number ratio $\geq$ 1.5 (amplification) was significantly higher in serous tumors ($p<0.0001$) and was associated with reduced survival duration ($p=0.0170$; Figure 1b).

We assessed the mechanisms by which amplification at 8q24 contribute to ovarian and breast pathophysiology by analyzing the effects of reducing expression levels of transcripts encoded in the region of recurrent amplification in cell lines with and without amplification at this locus. We identified ovarian cell lines amplified at this locus by applying array CGH (aCGH) to 30 ovarian cancer cell lines. Most regions of recurrent genome copy number abnormality including amplification at 8q24 in the cell lines were similar to those in primary serous ovarian tumors (Figure 1c and 1d) (21). The raw aCGH data has been deposited to http://www.ebi.ac.uk/cgi-bin/microarray/tab2mage.cgi, accession # E-TABM-246. Table S3 describes similarities in recurrent genome copy number abnormalities between the cell lines and primary tumors. Figures 1e and 1f show that the genome copy number profiles at 8q24 for several ovarian tumors and cell lines are similar and suggest a concensus region of amplification spanning ~1 Mbp encoding *MYC* and *PVT1*.

We also analyzed mRNA expression of ~17,000 transcripts using Affymetrix Hu_U133A GeneChip microarrays in the 30 ovarian cancer cell lines (Raw image .cel files and analyzed RMA data have been

deposited to http://www.ebi.ac.uk/cgi-bin/microarray/tab2mage.cgi, accession #E-TABM-254) and calculated Pearson's correlations between transcription levels and genome copy number changes in order to identify transcripts that were significantly deregulated by the genome copy number aberrations in the collection of cell lines. Each transcript was paired with a BAC clone that was nearest to the gene in the genome. These analyses revealed 417 transcripts with Pearson's correlations of >0.5 in both cell lines and in primary ovarian tumors (21) suggesting that the cell lines mirror much of the genome copy number driven transcriptional deregulation found in primary tumors. The genes are listed in supplementary Table S4. We used QPCR to analyze the expression levels of 57 transcripts (listed in Table S2) encoded in regions of recurrent copy number abnormality previously implicated in the pathophysiology of ovarian cancer. We analyzed these transcript levels in 21 cell lines (bold highlighted in Table S1) to determine the accuracy with which the microarray analyses estimated expression levels. Figure S1 shows correlation coefficients between QPCR and microarray results calculated for each gene in the 21 ovarian cancer cell lines. The correlation coefficients between expression levels measured using QPCR and Affymetrix array analysis were mostly high (average correlation coefficient 0.75) except for 5 genes including *PVT1* for which the correlation coefficients were very low to negative.

Since we observed some discordances between transcript levels measured using QPCR and Affymetrix expression array analysis, we measured transcript levels of the transcripts for PVT1 and MYC using QPCR in 20 ovarian cancer cell lines. The Affymetrixc U133A arrays used in this study carried probe sets 216240_at and 216249_at that were designed from EST clone M34428. The array signals for both probe sets were either undetectable or very low across all the lines whereas the Taqman analyses designed from the same source EST sequence detected significant and variable expression levels in the same cell lines (Table1). The Pearson's correlation between *PVT1* expression levels measured by microarray and by

QPCR was only -0.02 and -0.01 for 216240_at and 216249_at, respectively, while the correlation between *PVT1* transcript levels measured using QPCR and genome copy number at 8q24 was high (Table 1). We attribute these discordances to the poor performance of the probe sets for *PVT1* on the microarrays. Table 1 compares aCGH measurements of genome copy number at 8q24 and QPCR analyses of expression levels for *PVT1* and *MYC* in 20 of the ovarian cancer cell lines. Genome copy number was assessed at the BAC array probe closest to *PVT1* and *MYC* (clone VYS08A2679). The starting site of this BAC clone overlaps with 5' end of the *MYC* locus and 3' end of the clone is ~50kbp downstream of 5' end of the *PVT1* transcription unit. Both *PVT1* and *MYC* transcript levels were strongly correlated with genome copy number in the 20 ovarian cancer cell lines tested. Interestingly, the correlation between copy number and expression level was higher for *PVT1* than for *MYC*; 0.89 and 0.64, respectively. This is due to the fact that some cell lines (e.g. OVCA432 and OVCAR8) with amplification at 8q24 did not over express *MYC* while transcription levels of *PVT1* were high in all lines (e.g. CAOV4, HEY, OVCA432 and OVCAR8) showing amplification at 8q24. In most cell lines, transcription levels of *MYC* and *PVT1* were significantly higher where they were amplified than in cell lines in which they were not. However, *PVT1* was highly expressed in cell line TOV21G, even though it was not amplified suggesting another mechanism of over expression. We also compared transcription levels of *PVT1* in 18 different normal tissues, 3 breast cancer lines (SKBR3, HBL100 and SUM159T), and 2 normal ovarian cell lines (OSE1157 and IOSE29) to those in two 8q24 amplified ovarian cancer lines (CAOV4 and HEY) using QPCR. *PVT1* was expressed in several of the tissues tested with highest expression in trachea but not at levels found in the two ovarian cancer cell lines. Breast cell lines generally expressed *PVT1* at much lower levels than ovarian cells.

We preformed 5'RACE with cDNA from OSE1157, IOSE29, CAOV4 and HEY cells. Analyses of the intensities of bands generated by 5'RACE PCR products along with QPCR analyses showed that expression of *PVT1* in OSE1157 cells was significantly lower than that in IOSE29 cells and more than 20-fold lower than that in HEY and CAOV4 cells. Single bands of ~350 base pairs (bp) were only observed in 5'RACE PCR products from OSE1157 and HEY cells. The 5'RACE of IOSE29 and CAOV4 cells produced multiple bands. The single bands from OSE1157 and HEY cells were cut, gel purified, cloned into TOPO TA cloning vectors and sequenced with M13 primers flanking the inserted PCR products. Two different sequences (#1 and #2 in Figure S2) were obtained from OSE1157 5'RACE. Only one sequence was detected in plasmids isolated from 6 bacterial colonies that were transformed with 5'RACE PCR products from HEY cells. The HEY sequence was identical to the 5'RACE sequence #2 from OSE1157. We then searched human expressed sequence tag (EST) databases using NCBI Nucleotide-nucleotide BLAST (blastn) based on our 5'RACE sequences and the sequence of a cDNA clone (NCBI accession #: BC033263) that was previously considered to be a full-length clone for *PVT1*. The 125bp at the 3' ends of both 5'RACE sequences overlapped with the 5' end of the BC033263 sequence. ESTs that had over 95% sequence homology with the query sequences were assembled to predict full length transcripts. The web tool, NIX (Nucleotide Identify X software, http://www.hgmp.mrc.ac.uk/NIX), was used to identify exons from these EST alignments. Nine exons were predicted for each of the two *PVT1* full-length transcripts (Figure 2) assembled from sequences of 5'RACE #1 and #2 and BC033263. The two transcripts shared exons 2-9 but had different first exons. We termed the first exon that corresponds to 5'RACE sequence #1 as exon 1a and the exon that corresponds to 5'RACE sequence #2 as exon 1b. Exon 1a is upstream of exon 1b in the genome (Figure 2). In order to determine whether or not the predicted full-length transcripts exist in the transcriptome, primers against exon 1a or 1b and exon 9 were used to

amplify *PVT1* cDNAs from the HEY cells and normal testis. PCR products were then cloned and sequenced. As shown in Figure 2, multiple alternatively spliced variants were identified from these PCR products. Predicted exons 4 and 8 were missing in all of the 22 PCR products that we have cloned. We also assessed the sequences of individual *PVT1* exons detected by PCR for possible stem-loop structures that could signify the presence of transcripts that will be bound and cleaved by Drosha to liberate ~70nt miRNA precursors (22). Sequences homologous to known stem-loop structures in different species were found in predicted exons 5, 6, 7, and 9; however, the significance indices of these predictions were low in all cases.

Biological responses to inhibition of *PVT1* and *MYC* expression. Since our main goal in this study was to determine how *PVT1* and MYC contribute to ovarian cancer pathophysiology when over expressed by amplification or other genomic mechanisms, we compared biological responses to inhibition of *PVT1* and *MYC* in ovarian and breast cancer cell lines with and without amplification and over expression of these two genes.

We assessed the biological effects of inhibiting mRNA levels of *PVT1* using siRNAs in the ovarian cancer cell lines CAOV4, HEY, OVCA432 and OVCAR8 where 8q24 is amplified and *PVT1* is over expressed and in cell lines A2780, CAOV3, OV90 and SKOV3 where *PVT1* is not amplified or over expressed. We compared these responses to responses to siRNA inhibition of *MYC* expression in a subset of these lines. After 48 h, more than 50% knock-down in *PVT1* mRNA level was achieved in all ovarian cancer lines treated with 120nM siPVT1a and at least 80% knock-down was achieved in HEY cells treated with either 120nM siPVT1a or siPVT1b. Representative semi-quantitative RT-PCR agarose gel electrophoresis and Taqman® QPCR analyses of *PVT1* are shown in Figures 3a and 3b, respectively.

Figure 3a also shows similar *PVT1* knock-down levels in three breast cancer cell lines (SUM159PT, HBL100 and SKBR3). Notably, siRNA knockdown of *PVT1* expression was accompanied by a slight decrease in *MYC* protein expression in CAOV4 but not in any of the other cell lines (Figure 3c). Figure 3c shows that 200nM siMYCa also reduced the level of *MYC* protein expression to >50% at 48h. In order to minimize off-target effects of high concentration of siRNA, we also assessed responses to a different siRNA against *MYC* (siMYCb) that reduced the *MYC* mRNA level in HEY cells to less than 12% of that in siControl transfected cells (Figure 3d) at 120nM. Eight other siRNAs targeting different parts of *PVT1* transcript (see Figure 2) were also tested for knock-down in HEY cells but none of these reduced *PVT1* mRNA levels significantly.

Knock-down *of PVT1 and MYC inhibits proliferation***.** We determined the effects of *PVT1* and/or *MYC* knock-down on cell proliferation by measuring changes in fractions of cells in the G_1-, S- and G_2M-phases of the cell cycle estimated from BrdUrd/DNA distributions measured for cells pulse labeled with BrdUrd at 8, 24 and/or 48 h after siRNA transfection and by counting viable cells using the CTG assay that measures ATP levels in metabolically active cells. Table 2 shows that siPVT1a strongly inhibited BrdUrd incorporation in four *PVT1*-amplified/over expressed cell lines but not in any of the non-amplified lines at 48 h. In HEY and OVCAR8, the reduction in the fraction of cells in S-phase was accompanied by a significant accumulation of cells in G_1-phase of the cell cycle. Treatment with 120nM siPVT1a and 200nM siMYCa produced similar levels of inhibition of BrdUrd incorporation in CAOV4 and HEY cells in which both *PVT1* and *MYC* are amplified and over expressed (Table 2). Neither G_1 cell cycle arrest nor reduction in S-phase was seen in any of the four *PVT1/MYC* non-amplified/over expressed cell lines. siPVT1b had even stronger anti-proliferation effects in CAOV4 and HEY cells than siPVT1a (Table 2). We also evaluated the effect of siRNA knock-down with siPVT1a on cell growth

using CTG assays. Table 2 shows that the number of viable cells in siPVT1a transfected HEY cells started to decrease relative to that of cells treated with Lipofectamine alone or siControl at 8 h. By 24 h, the viable cell count was only 40% of that of control cultures. In contrast, siPVT1a had no effect on cell viability in two ovarian cell lines in which *PVT1* was not amplified or over expressed.

In order to determine the generality of the phenotype resulting from *PVT1* knock-down, we also compared the effect of siPVT1a transfection in two breast cancer cell lines (SUM159PT and HBL100) in which *PVT1* is both amplified and over expressed with that in a breast line (SKBR3) where *PVT1* is only amplified but not over expressed. As shown in Table 2, transfection of siPVT1a decreased the proportion of BrdUrd incorporating cells in SUM159PT and HBL100 but not in SKBR3.

Knock-down of PVT1 but not MYC increases apoptosis. We assessed the effects of inhibiting *PVT1* expression on programmed cell death in cells with and without *PVT1* amplification/over expression by measuring membrane permeability (23), cell morphology and F-actin reorganization (24, 25) using high content image analyses. Yo-Pro®-1 dye uptake increases when cells lose membrane integrity during cell death while F-actin reorganization resulting in increased Alexa Fluor® 488 Phalloidin binding that has been associated with earlier stages of apoptosis (25). Beginning at 8 h after transfection, siPVT1a significantly increased Yo-Pro®-1 dye uptake and F-actin staining relative to Lipofectamine controls in HEY and CAOV4 cell lines in which *PVT1* is amplified and over expressed (Figure 4a and 4b). Increased apoptosis in siPVT1a transfected cells was further confirmed with Annexin V staining in CAOV4 cells (data not shown). In contrast, transfection of siPVT1a in 3 of the 4 non-amplified/over expressed lines produced no significant changes except in SKOV3 cells where F-actin staining increased significantly after siPVT1a transfection ($p=0.001$). Apoptosis induced by siRNA knock-down of *PVT1* expression was more pronounced in CAOV4 and HEY cells transfected with siPVT1b as compared to cells transfected

with siPVT1a. No effect on apoptosis was seen in the non-amplified cell line, OV90, transfected with either siPVT1a or siPVT1b (Figure 4c). Transfection with 120nM siMYCb did not significantly affect apoptosis in any of the cell lines tested (Figure 4b and 4c). Increased apoptosis was also seen in the breast cancer cell lines in which *PVT1* was amplified and over expressed following transfection of siPVT1a, but not in SKBR3 where *PVT1* was not over expressed (data not shown). We also treated the 8 ovarian cell lines with Paclitaxel as a positive control for apoptosis induction. 100nM Paclitaxel induced massive apoptosis in 6 of the 8 cell lines as expected with the exception of two PVT1 amplified/over expressed cell lines (HEY and OVCA432) (Figure 4a).

DISCUSSION

Several published findings implicate *PVT1* in aspects of cancer pathophysiology. Examples include observations that rearrangement of the region at 8q24 encoding *MYC* and *PVT1* is frequently involved in human leukemias and lymphomas (4, 5), the regions is frequently amplified in solid tumors (2) and a site of recurrent tumorigenic viral integration in mice (26). *MYC* is well established as an oncogene in this region. We now provide functional evidence for the importance of increased expression of *PVT1* in cancer through analysis of cell lines with and without amplification at 8q24. These cell lines were selected from a collection of 30 ovarian cell lines described in this paper and 51 breast cancer cell lines described elsewhere (11). Our analyses of both collections show that the recurrent genome aberrations and the resulting deregulation of gene expression are highly concordant between primary tumors and the cell lines. Thus, the aspects of amplification dependent cancer pathophysiology discovered in the cell lines are likely to be obtained in primary tumors as well.

The strongest evidence for the importance of *PVT1* in cancer pathophysiology is our observation that siRNA silencing of *PVT1* expression decreases cell proliferation and increases apoptosis in breast and ovarian cancer cell lines in which it was amplified and over expressed but not in cell lines where it is not amplified/over expressed. The amplification/over expression-specific response phenotypes argue that the observed effects are due to down regulation of *PVT1* rather than to off-target effects of siRNA. The *PVT1* specificity of the response is further supported by our observation that the same amplification/over expression-specific response phenotype was seen using two different siRNAs against *PVT1*.

PVT1 has been suggested to function as a *MYC* activator. However, our demonstration that *PVT1* inhibition does not alter *MYC* levels in most of the cell lines where it influences both apoptosis and proliferation argues against this. Moreover, inhibition of *PVT1* but not *MYC* induces apoptosis in cell lines where they are both amplified and over expressed. If *PVT1* were acting through *MYC*, the apoptotic response should have been observed after inhibition of *MYC*. Therefore, we conclude that *PVT1* acts independently of *MYC* in generation of the apoptotic phenotype.

The strong induction of apoptosis resulting from siRNA inhibition of *PVT1* suggests that *PVT1* amplification contributes to the oncogenic phenotype, at least in part by suppressing apoptosis. This suggests the interesting possibility that amplification at 8q24 might have two simultaneous oncogenic functions: over expression of *MYC*, which stimulates proliferation, and over expression of *PVT1,* which not only stimulates proliferation but also inhibits the apoptotic response normally associated with over expression of *MYC*. The apoptosis suppression function of *PVT1* may also explain why its over expression is associated with reduced survival duration in patients treated with platinum plus taxane-based therapies. Platinum compounds produce apoptotic responses through production of DNA cross-

links (27) while taxanes, trigger apoptotic responses by stabilizing otherwise dynamic microtubules that are important for centrosome and mitotic spindle function (28). Over expression of *PVT1* may contribute to resistance to these agents by suppressing the apoptotic mechanisms through which they work. This possibility is partially supported by our finding that two ovarian cancer cell lines with high level *PVT1* expression do not exhibit significant apoptotic responses to treatment with paclitaxel at concentrations that induced apoptosis in the other cell lines. However, *PVT1* is not the only determinant of response since two other *PVT1* amplified/over expressed cell lines exhibit a significant apoptotic response to paclitaxel.

Elucidation of the mechanism(s) by which *PVT1* over expression contributes to suppression of apoptosis and proliferation is complicated by the fact that *PVT1* is transcribed into multiple splice forms that vary in form and abundance between cell lines (data not shown and (9)). However, our observation that siRNAs complementary to sequences in exons 2 and 3 both produced phenotypes that were specific to cell lines with amplification and over expression of *PVT1* suggested that transcripts containing these two exons are functionally important.

Mechanistic interpretation is further complicated by the observation that *PVT1* appears to be a ncRNA since the longest open reading-frame predicted from our assessment of *PVT1* sequences is 150 amino acids encoded in the first two exons. The ncRNAs most strongly implicated in cancer so far are miRNAs (29). These 20-22 nucleotide RNAs are the result of enzymatic processing of larger transcripts and may operate in cancer by blocking translation of target genes to which they are complementary. Deregulated expression of several miRNAs has been associated with poor disease outcome in chronic lymphocytic leukemia, colorectal neoplasia, lung cancer and Burkitt lymphoma (29). miRNAs are also frequently

located at fragile sites and genomic regions that are involved cancers (30). Thus, we investigated the possibility of *PVT1* as a miRNA. Our computational analyses show that the predicted sequences of *PVT1* transcripts do not seem to have the 'stem-loop' structures normally associated with miRNAs (20, 31, 32). A recent study by Dr. Huppi has identified 7 putative miRNAs within the ~400kb *PVT1* genomic locus (Private communication). The precursor sequence of one of these overlaps with exon 1b in our current study, but it also extends beyond the consensus splice site of the exon. The precursor sequences of the other 6 miRNAs have no association with any of the annotated *PVT1* exons and might be results of extensive alternative splicing found in this locus (Figure 2 and communications with Dr. Konrad Huppi). This may explain our failure to identify potential miRNAs precursor sequences in our predicted *PVT1* transcripts, which contain mostly known exons. Thus, the mechanism by which *PVT1* exerts its pathological function remains unclear.

In conclusion, we have used our well-characterized cell line collection to demonstrate that amplification at 8q24 increases expression of both *MYC* and *PVT1* and that both of these deregulated transcripts appear to contribute to ovarian and breast cancer pathophysiology. We have demonstrated that *PVT1* is most likely an ncRNA that acts independently of *MYC* and when amplified and over expressed, acts to increase proliferation and inhibit apoptosis.

REFERENCES

1. Lancaster JM, Dressman HK, Whitaker RS*, et al.* Gene expression patterns that characterize advanced stage serous ovarian cancers. J Soc Gynecol Investig 2004;11(1):51-9.

2. Popescu NC, Zimonjic DB. Chromosome-mediated alterations of the MYC gene in human cancer. J Cell Mol Med 2002;6(2):151-9.

3. Shtivelman E, Henglein B, Groitl P, Lipp M, Bishop JM. Identification of a human transcription unit affected by the variant chromosomal translocations 2;8 and 8;22 of Burkitt lymphoma. Proc Natl Acad Sci U S A 1989;86(9):3257-60.

4. Cory S, Graham M, Webb E, Corcoran L, Adams JM. Variant (6;15) translocations in murine plasmacytomas involve a chromosome 15 locus at least 72 kb from the c-myc oncogene. Embo J 1985;4(3):675-81.

5. Webb E, Adams JM, Cory S. Variant (6 ; 15) translocation in a murine plasmacytoma occurs near an immunoglobulin kappa gene but far from the myc oncogene. Nature 1984;312(5996):777-9.

6. Graham M, Adams JM, Cory S. Murine T lymphomas with retroviral inserts in the chromosomal 15 locus for plasmacytoma variant translocations. Nature 1985;314(6013):740-3.

7. Graham M, Adams JM. Chromosome 8 breakpoint far 3' of the c-myc oncogene in a Burkitt's lymphoma 2;8 variant translocation is equivalent to the murine pvt-1 locus. Embo J 1986;5(11):2845-51.

8. Mengle-Gaw L, Rabbitts TH. A human chromosome 8 region with abnormalities in B cell, HTLV-I+ T cell and c-myc amplified tumours. Embo J 1987;6(7):1959-65.

9. Shtivelman E, Bishop JM. The PVT gene frequently amplifies with MYC in tumor cells. Mol Cell Biol 1989;9(3):1148-54.

10. Shtivelman E, Bishop JM. Effects of translocations on transcription from PVT. Mol Cell Biol 1990;10(4):1835-9.

11. Neve RM, Chin K, Fridlyand J*, et al.* A collection of breast cancer cell lines for the study of functionally distinct cancer subtypes. Cancer Cell 2006;10(6):515-27.

12. Hodgson G, Hager JH, Volik S*, et al.* Genome scanning with array CGH delineates regional alterations in mouse islet carcinomas. Nat Genet 2001;29(4):459-64.

13. Hackett CS, Hodgson JG, Law ME*, et al.* Genome-wide array CGH analysis of murine neuroblastoma reveals distinct genomic aberrations which parallel those in human tumors. Cancer Res 2003;63(17):5266-73.

14. Snijders AM, Nowak N, Segraves R*, et al.* Assembly of microarrays for genome-wide measurement of DNA copy number. Nat Genet 2001;29(3):263-4.

15. Lapuk A, Volik S, Vincent R*, et al.* Computational BAC clone contig assembly for comprehensive genome analysis. Genes Chromosomes Cancer 2004;40(1):66-71.

16. Irizarry RA, Bolstad BM, Collin F, Cope LM, Hobbs B, Speed TP. Summaries of Affymetrix GeneChip probe level data. Nucleic Acids Res 2003;31:(4,e15).

17. Ginzinger DG. Gene quantification using real-time quantitative PCR: an emerging technology hits the mainstream. Exp Hematol 2002;30(6):503-12.

18. Stilwell JL, Guan Y, Neve RM, Gray JW. Systems biology in cancer research: genomics to cellomics. Methods in molecular biology 356:353-65.

19. Griffiths-Jones S. The microRNA Registry. Nucleic acids research 2004;32(Database issue):D109-11.

20. Griffiths-Jones S, Grocock RJ, van Dongen S, Bateman A, Enright AJ. miRBase: microRNA sequences, targets and gene nomenclature. Nucleic acids research 2006;34(Database issue):D140-4.

21. Kuo W-L, Fridlyand J, Novak B*, et al.* Genomic deregulation of transcription in serous ovarian cancers; prognostic markers and therapeutic targets. Cancer Res 2006;(submitted).

22. Murchison EP, Hannon GJ. miRNAs on the move: miRNA biogenesis and the RNAi machinery. Curr Opin Cell Biol 2004;16(3):223-9.

23. Mingeot-Leclercq MP, Brasseur R, Schanck A. Molecular parameters involved in aminoglycoside nephrotoxicity. J Toxicol Environ Health 1995;44(3):263-300.

24. Levee MG, Dabrowska MI, Lelli JL, Jr., Hinshaw DB. Actin polymerization and depolymerization during apoptosis in HL-60 cells. Am J Physiol 1996;271(6 Pt 1):C1981-92.

25. Okada T, Otani H, Wu Y*, et al.* Role of F-actin organization in p38 MAP kinase-mediated apoptosis and necrosis in neonatal rat cardiomyocytes subjected to simulated ischemia and reoxygenation. Am J Physiol Heart Circ Physiol 2005;289(6):H2310-8.

26. Akagi K, Suzuki T, Stephens RM, Jenkins NA, Copeland NG. RTCGD: retroviral tagged cancer gene database. Nucleic acids research 2004;32(Database issue):D523-7.

27. Cepeda V, Fuertes MA, Castilla J, Alonso C, Quevedo C, Perez JM. Biochemical mechanisms of cisplatin cytotoxicity. Anti-cancer agents in medicinal chemistry 2007;7(1):3-18.

28. Bergstralh DT, Ting JP. Microtubule stabilizing agents: their molecular signaling consequences and the potential for enhancement by drug combination. Cancer Treat Rev 2006;32(3):166-79.

29. Gregory RI, Shiekhattar R. MicroRNA biogenesis and cancer. Cancer Res 2005;65(9):3509-12.

30. Calin GA, Sevignani C, Dumitru CD*, et al.* Human microRNA genes are frequently located at fragile sites and genomic regions involved in cancers. Proc Natl Acad Sci U S A 2004;101(9):2999-3004.

31. McManus MT. MicroRNAs and cancer. Semin Cancer Biol 2003;13(4):253-8.

32. Mattick JS, Makunin IV. Non-coding RNA. Hum Mol Genet 2006;15 Spec No 1:R17-29.

A**CKNOWLEDGEMENT**

We thank Dr. Richard E. Neve, Dr. Eric A. Collisson, Dr. Konrad Huppi and Dr. Natasha J Kaplen for helpful discussions. We gratefully acknowledge receipt of a pre-publication copy of Dr. Huppi's manuscript on PVT1 miRNAs. This work was supported by the NIH (CA 58207, CA83639 and CA 64602) and the Office of Health and Environmental Research of the U.S. Department of Energy (Contract DE-AC03-76SF00098). The content of this publication does not necessarily reflect the views or policies of the Department of Health and Human Services, nor does mention of trade names, commercial products, or organization imply endorsement by the U.S. Government.

FIGURE AND TABLE LEGENDS

Figure 1. Recurrent copy number aberrations in ovarian tumors and cell lines. (**a)** Relative amplification of the chr8q24 locus determined using FISH with a spectrum orange labeled probes for MYC (red) and a spectrum green labeled probe for centromere of chromosome 8 (green) in a mucinous tumor case (probes from Vysis, Downers Grove Ill). The ratio of the number of copies of the MYC probe relative to the number of copies of centromere 8 was 6.8 in this case indicating high level of amplification. (**b)** Kaplan-Meyer plot showing survival rates in 380 stage I-III ovarian tumors with and without amplification of chr8q24 detected by FISH. **(c) and (d)** Frequencies of significant increases or decreases in genome copy numbers are plotted as a function of genome distances of UCSC July, 2003 freeze (NCBI Build 34) for 30 cell lines **(c)** and primary tumors from Study B of Kuo et al(21) (**d)** Positive values indicate frequencies of samples showing copy number increases and negative values indicate frequencies of samples showing copy number decreases**.** The gray bars show the frequencies of $\log_2$ copy numbers >0.3 or <-0.3 and the black bars show the frequencies of $\log_2$ copy numbers >0.9 or <-0.9. The solid vertical gray lines indicate chromosome boundaries and dotted vertical lines indicate centromere locations. The numbers of the even-numbered chromosomes are marked at the bottom of each graph. Data are arranged with chromosome 1pter to the left and chromosomes Xqter to the right. (**e)** Log_2 copy number changes in 7 ovarian cell lines that had amplification on chromosome 8q24. **(f)** Log_2 copy numbers in ovarian tumors (21) showing copy number increases at 8q24. The *MYC/ PVT1* amplicon was defined by the minimal overlapping regions from tumors as shown.

Figure 2 Genomic mapping of PVT1 transcripts identified from HEY cells and normal testis and alignment of siRNAs against PVT1. The chromosome distance coordinates in kbp from NCBI Build 36.2 of the *PVT1* locus were marked at the bottom of the graph. Each box represents a segment of cDNA sequence from a transcript, and the lines in between represent genomic sequence. The arrow at the end of

each transcript points to the direction of transcription, which in all cases are in the sense direction. Transcripts A1-A11 are PCR products amplified with primers against predicted exon 1a and exon 9. Transcripts B1-B11 are PCR products amplified with primers against predicted exon 1b and exon 9. The positions of the 5'RACE sequences #1 and #2 and the EST clone BC033263 are also mapped for reference. The position of 9 predicted exons from full-length transcript A and transcript B are marked on top of the map. The predicted exons 2, 3 and 7 are magnified to show alignments of *PVT1* siRNAs. The block arrowheads represent the siPVT1a and siPVT1b used in this study that have shown significant knock-down of *PVT1* mRNA levels in multiple cell lines. Light gray horizontal lines represent other siRNAs that did not show significant knock-down of *PVT1* transcription.

Figure 3 Expression of *PVT1* and *MYC* in control and siRNA treated cells. (**a**) Agarose gel electrophoresis images of semi-quantitative RT-PCR specific for *PVT1* transcript in CAOV4, HEY, SUM159PT, HBL100 and SKBR3 cells treated with conditions as indicated. GUS expression was tested as the sample loading control. (**b**) % *PVT1* mRNA level knock-down measured by Taqman® QPCR in HEY cells transfected with 3 concentrations (as indicated in the graph) of siPVT1a and siPVT1b as compared to cells transfected with siControl. (**c**) Western blots with anti-*MYC* antibody in CAOV4 and HEY cells transfected with siPVT1a and siMYCa. In these experiments, the Null control was cells that were incubated with Opti-MEM only during transfection. The Lipo control was cells that were mock-transfected with Lipofectamine 2000 at a maximum concentration used in each experiment (5-7.5mg/ml). **(d)** % *MYC* mRNA level knock-down measured by Taqman® QPCR in HEY cells transfected with different concentrations (as indicated in the graph) of siMYCb as compared to cells treated with siControl.

Figure 4 Effects of *PVT1* and *MYC* siRNAs on apoptosis in ovarian and/or breast cancer cell lines measured by the Cellomics HCS system. **(a)** Cell permeability (Yo-Pro®-1 dye intake) and microfilament reorganization (F-actin staining) in *PVT1* amplified/over expressed and non-amplified ovarian cell lines treated with siPVT1a and Paclitaxel for 48 h. For the amplified lines, the white bars represent data from CAOV4, the bars with black stripes are for HEY, the dotted bars are for OVCA432 and the solid black bars represent results from OVCAR8. For non-amplified cell lines, the gray bars represent data from A2780, the bars that have white hatched stripes against a black background represent CAOV3, the bars with checkered pattern are for OV90 and the bars with cross-hatched lines represent data from SKOV3. **(b)** Apoptosis induced by transfection of 120nM siPVT1a at 8, 24 and 48 h in *PVT1* amplified/over expressed and non-amplified ovarian cell lines. All the siRNAs was tranfected at 120nM concentration. The heights of the columns in bar graphs represent fold changes in apoptotic cell proportions from Lipofectamine (Lipo) treated cells. * indicates experiments in which the difference in total fluorescent intensity was significant between siPVT1a transfected cells and Lipo treated control cells ($p<0.05$). **(c)** Comparison of apoptotic effects (measured by Yo-Pro®-1 dye intake) induced by 120nM siPVT1a and siPVT1b transfection at 48 h in three ovarian cell lines.

Table 1 Expression levels of *PVT1* and *MYC* and genome copy number changes at 8q24 in ovarian cancer cell lines.

Table 2 Effects of *PVT1* and *MYC* siRNAs on cell proliferation in ovarian and/or breast cancer cell lines. BrdUrd/PI cell cycle distributions were measured by FACS analyses or Cellomics® High Content imaging. Viable cell counts were assessed using the CellTiter-Glo® Luminescent cell viability assay. Lipo: Lipofectamine

SUPPLEMENTARY MATERIALS

Figure S1 Correlation of gene expression levels tested by Taqman® QPCR and Affymetrix oligonucleotide U133A arrays

Figure S2 Nucleotide sequences of two PCR products from 5'RACE in OSE1157 cells

Table S1 List of ovarian cancer cell lines used in the study

Table S2 List of genes tested in Taqman® QPCR assays

Table S3 Gene copy numbers in 30 ovarian cell lines in genomic regions that were amplified or deleted in more than 20% ovarian tumors from study A and B of Kuo et al (21). All the aCGH BAC clones listed in this table had gained or lost at least one copy ($\log_2$ ratio>0.5 or <-0.5) in tumors from study A or B. Red boxes indicate gains of at least one copy and green boxes indicates losses of at least one copy. Dark red indicates high level amplification ($\log_2$ ratio >3) and dark green indicates homozygous deletions ($\log_2$ ratio < -2)

Table S4 List of genes of which expression was regulated by gene copy numbers in both ovarian tumors and cell lines

Figure 1 (Guan Y. *et al*)

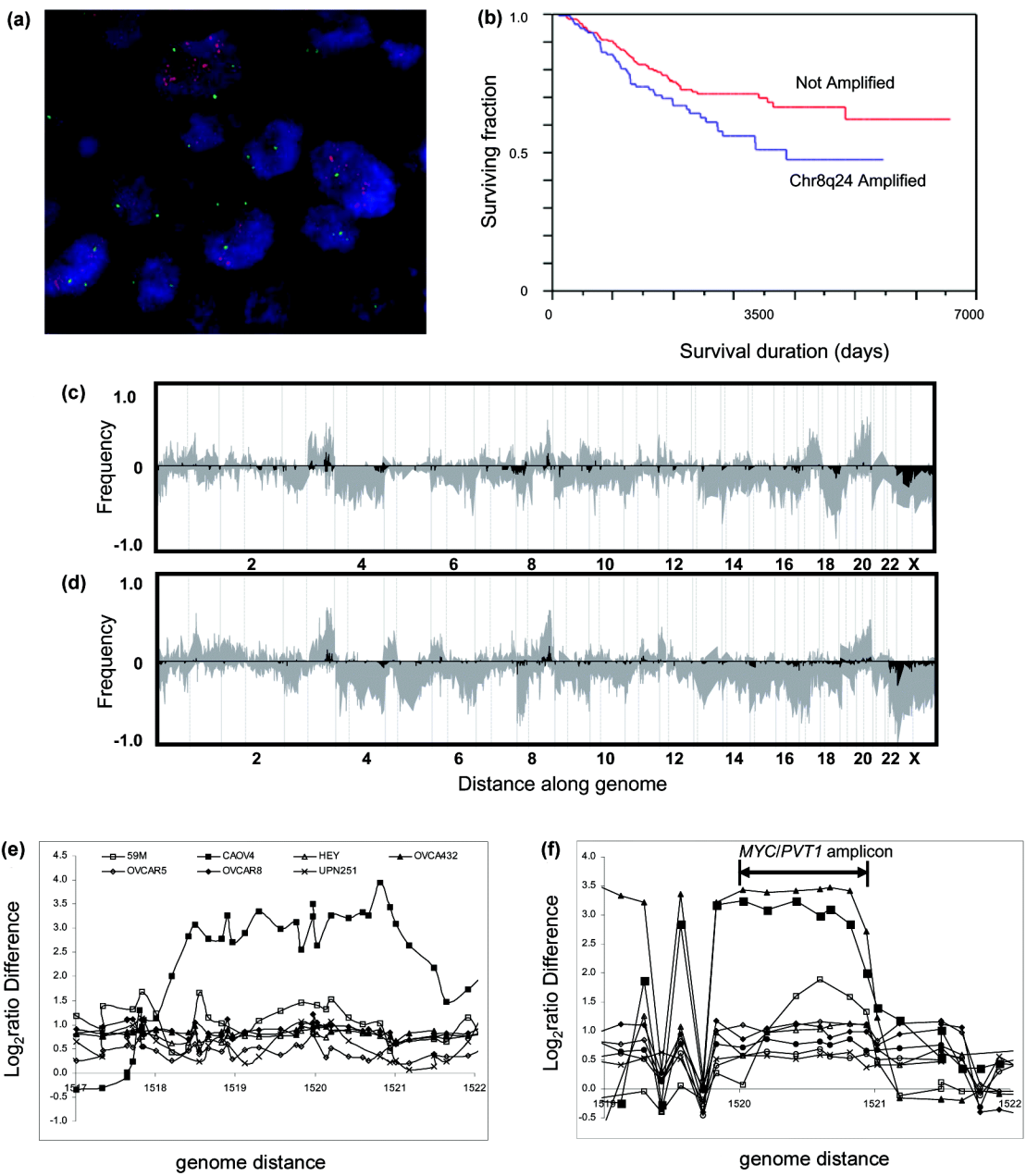

Figure 2 (Guan Y. *et al*)

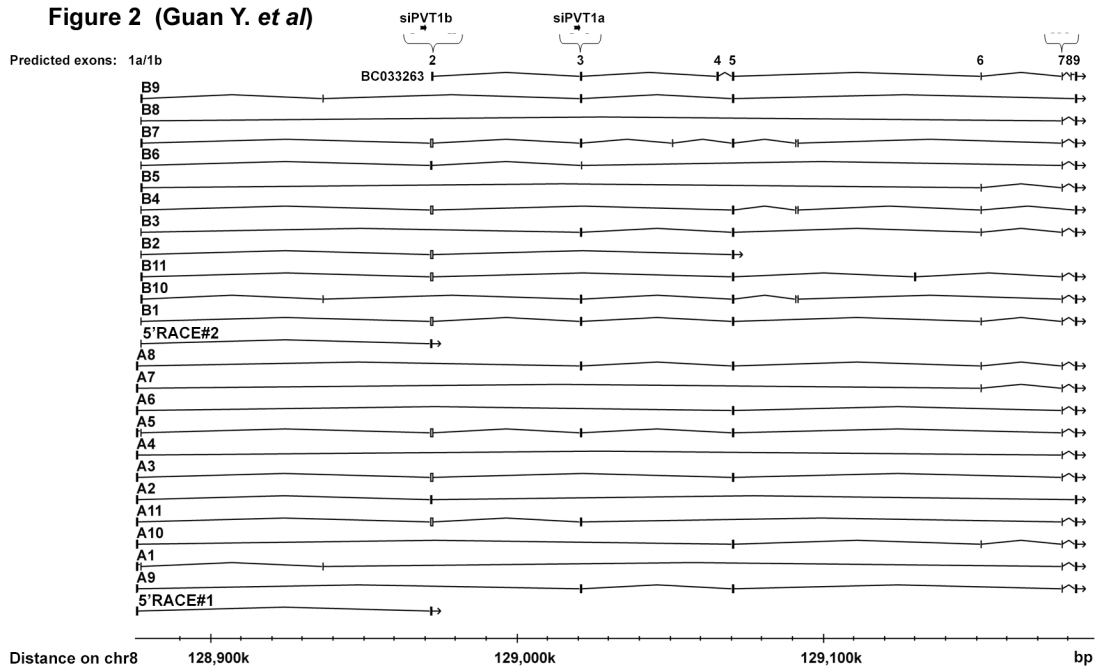

Figure 3 (Guan Y. *et al*)

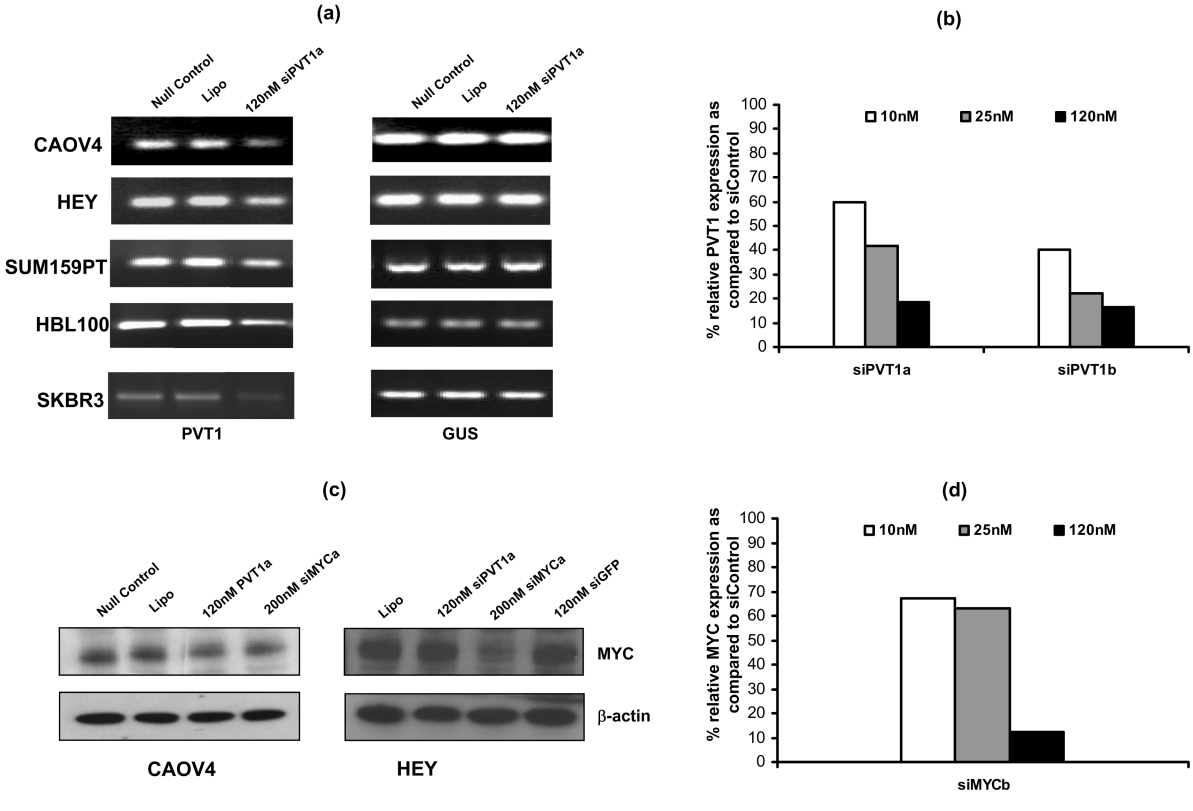

Figure 4 (Guan Y. *et al*)

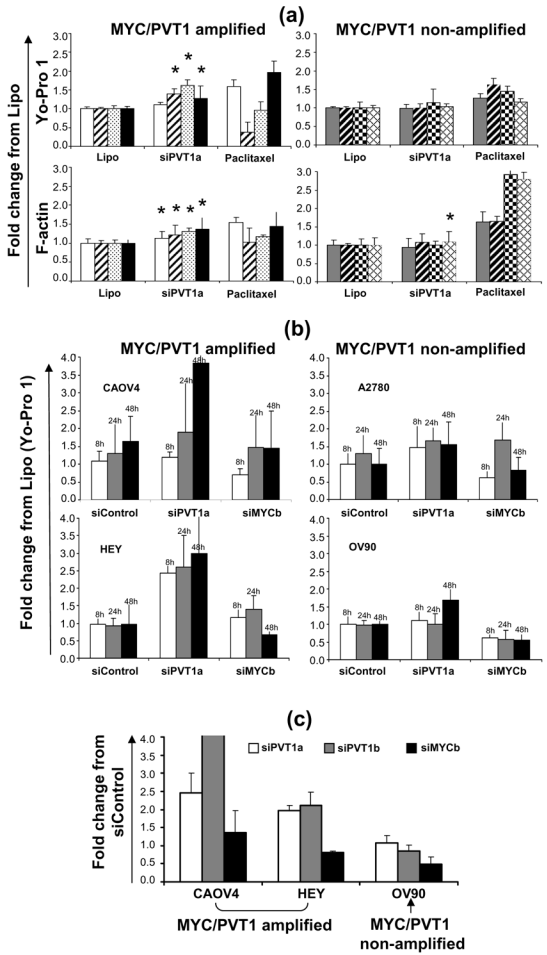

Table1 (Guan Y. *et al*)

cell line name	PVT1	clone VYS08A2679	c-myc
	Taqman expression (normalized to the expression of Stratagen RNA Reference Pool)	copy number changes	Taqman expression (normalized to the expression of Stratagen RNA Reference Pool)
A2780	0.91	-0.17	1.14
CAOV3	0.91	-0.04	0.09
CAOV4*	21.36	3.15	2.49
DOV13	2.05	-0.07	0.60
ES-2	1.29	0.32	0.86
HEY*	5.09	0.63	2.88
OCC1	0.67	-0.44	0.30
OV90	0.25	-0.02	0.62
OVCA 420	1.89	0.54	1.92
OVCA429	3.28	0.09	0.72
OVCA432*	7.18	0.91	1.25
OVCA433	3.14	0.04	0.62
OVCAR3	1.47	0.52	0.45
OVCAR5	2.93	0.73	1.24
OVCAR8*	3.54	1.09	1.00
PA-1	2.55	-0.01	0.80
SKOV3	0.70	0.09	0.76
SW626	1.95	0.22	1.63
TOV112D	1.25	0.40	1.19
TOV21G	5.74	0.00	0.82
correlation coefficency	r^2=0.89		r^2=0.64

*: Cell lines with both overexpression and amplification of *PVT1*

Table 2 (Guan Y. *et al*)

BrdUrd cell cycle FACS analysis

average % distribution (n=2 or 3)

MYC/PVT1 amplified		Lipo	120nM siGFP	120nM siPVT1a	200nM siMYCb
CAOV4	G_1	56	48	60	56
	S	17	19	2	7
HEY	G_1	44		66	61
	S	41		1	4
OVCA432	G_1	36	43	53	
	S	39	33	9	
OVCAR8	G_1	25	26	57	
	S	42	45	3	
MYC/PVT1 non-amplified		Lipo	120nM siGFP	120nM siPVT1a	200nM siMYCb
A2780	G_1	33	31	35	
	S	49	49	48	
CAOV3	G_1	58	60	58	
	S	24	21	22	
OV90	G_1	51		47	43
	S	32		30	35
SKOV3	G_1		39	42	
	S		17	17	

CTG assay

average % viable cell count vs Lipo control (n=4)

MYC/PVT1 amplified		120nM siControl	120nM siPVT1a
HEY	8h	104	64
	24h	86	40
	48h	104	45
MYC/PVT1 non-amplified		120nM siControl	120nM siPVT1a
A2780	8h	100	107
	24h	97	144
	48h	92	98
OV90	8h	100	111
	24h	107	105
	48h	106	104

Cellomics® BrdUrd incorporation assay

averege % BrdUrd proportion (S-phase) (n=4)

PVT1 overexpressed	120nM siControl	120nM siPVT1a	120nM siPVT1b	120nM siMYCb
CAOV4	34	12	0.4	9
HEY	30	4	3	
SUM159PT	52	16		
HBL100	21	11		
PVT1 non-overexpressed	120nM siControl	120nM siPVT1a	120nM siPVT1b	120nM siMYCb
OV90	12	30	23	14
SKBR3	16	19		